Journal of Chromatography A, 1576 (2018) 131–136

Contents lists available at ScienceDirect

Journal of Chromatography A

journal homepage: www.elsevier.com/locate/chroma

Investigation of steric transition with field programming in frit inlet asymmetrical flow field-flow fractionation

Young Beom Kim, Joon Seon Yang, Myeong Hee Moon*

Department of Chemistry, Yonsei University, 50 Yonsei-ro, Seoul, 03722, South Korea

ARTICLE INFO

Article history:
Received 16 July 2018
Received in revised form 6 September 2018
Accepted 16 September 2018
Available online 18 September 2018

Keywords:
Frit inlet asymmetrical flow field-flow fractionation (FI-AF4)
Steric transition
Field programming
Particle separation

ABSTRACT

Steric transition in flow field-flow fractionation (FlFFF) was investigated under field programming by varying the channel thickness of a frit inlet asymmetrical FlFFF (FI-AF4). Steric transition is a typical inversion in sample elution mode from the increasing order of diameter (normal mode) to the opposite order (steric mode). Owing to the co-elution of two different-sized particles in the steric transition region where particles elute by the combination of the two elution modes, a loss of information in determining the accurate size of sample components in field-flow fractionation occurs. In this study, the effect of field programming on the steric transition in FI-AF4 was examined with the increase in channel thickness in order to increase the diffusional contribution of particle retention with the simultaneous reduction of steric contribution. This study demonstrated that the steric inversion diameter can be increased to >1 μm by programming the crossflow rate and by increasing the channel thickness to 350 and 490 μm. The present study also investigated the effects of outflow rate and initial field strength on the particle separation in field-programmed FI-AF4.

1. Introduction

Field-flow fractionation (FFF) refers a group of elution-based separation methods utilizing external forces to retain particles or macromolecules in an empty channel with a migration flow having parabolic velocity profiles [1,2]. Flow FFF (FlFFF), a sub-technique of FFF, employs a secondary flow as an external force that moves across the channel in the direction perpendicular to migration flow [3]. FlFFF is the most widely used technique among FFF methods owing to its various applications to macromolecules whose sizes range from 1000 Da to ~ 50 μm including water soluble polymers, organic polymers, proteins, cells, subcellular species, and particulate materials [4–10].

The size separation of particles by FFF is generally based on the interaction of particles with external forces. When particles are pushed toward one wall of a channel (accumulation wall) by external forces (sedimentation force in sedimentation FFF or crossflow in FlFFF), submicron-sized particles find an equilibrium between the two counter-directing forces (the external force and Brownian diffusion) in such a way that smaller particles protrude away from the channel wall toward the faster streamline region of parabolic flow profiles whereas larger particles find the equilibrium position close to the wall. Therefore, smaller particles elute earlier than the larger ones, which is called the normal mode of retention [2]. However, particles larger than a certain size limit exhibit negligible diffusion, but are elevated to a finite distance against the channel wall by hydrodynamic lift forces. In this case, the center of larger particles is exposed to a faster streamline than that of smaller ones, and therefore, larger particles migrate faster. The latter is referred to as the steric mode of retention [11]. In between the two retention modes, there is a particle size range called the steric transition region, where particle retention is governed by the combination of both normal and steric modes, and the particle size with the longest retention time in both retention modes is called the steric inversion diameter [12]. In the steric transition region, particles of two different sizes around the steric inversion diameter elute together, which often makes it difficult to determine accurate sizes. The steric inversion diameter can be varied by controlling the field strengths and flow rate in FFF. Its typical value was reported as ~1 μm for polystyrene (PS) latex particles in sedimentation FFF (SdFFF) [13] and 0.4–0.5 μm for FlFFF including cylindrical channel system as in hollow fiber FlFFF (HF5) [14–16]. In FlFFF, large particles elute by the steric/hyperlayer mode of elution in which the migration height of particle increases with the particle size so that larger particles migrate at a distance further away from the bottom height

* Corresponding author.
E-mail address: mhmoon@yonsei.ac.kr (M.H. Moon).

https://doi.org/10.1016/j.chroma.2018.09.036
0021-9673/

of smaller particles, resulting in a decrease in the steric inversion diameter.

In analyzing sample materials with a broad size distribution by FFF, an optimized run condition needs to be selected for the successful size-based separation without encountering steric transition during run. Studies have shown that the steric inversion diameter can be decreased by increasing the field strength and flow rate simultaneously. The smallest value was reported as 0.22 μm for gold particles in SdFFF [13] and ~0.23 μm for PS latex in FlFFF [14]. Steric inversion diameter can be increased to a large diameter scale either by increasing the diffusional contribution or by reducing the influence of hydrodynamic lift forces on retention. The former effect can be achieved by increasing either the channel thickness or the temperature. An increase in the temperature during the separation was observed to result in an increase in steric inversion diameter up to ~0.8 μm at 73 °C for HF5 [16]. However, the latter effect can be obtained by employing field programming, which results in a substantial decrease in the hydrodynamic lift forces. A recent study shows that ultrahigh-molecular-weight copolymers in the range 10^7–10^8 Da can be resolved in either normal or steric/hyperlayer mode by adjusting the decay patterns of field programming in a frit inlet AF4 (FI-AF4) channel system [17]. However, it is not clear yet how large the steric inversion diameter can be extended in case of particle separation by FlFFF, especially using FI-AF4 channel system. An FI-AF4 channel utilizes a short (~ 3 cm long) inlet frit at the beginning of the depletion wall of the typical AF4 channel so that sample components introduced to the channel are hydrodynamically compressed toward the accumulation wall by the incoming high-speed frit flow while they are migrating [18,19]. Therefore, sample relaxation in FI-AF4 can be continuously achieved without stopping the migration flow typically required for the focusing/relaxation procedure of AF4 and the possible sample adsorption by the accumulation wall can be reduced. In practice, hydrodynamic relaxation in FI-AF4 along with field-programmed separation has been useful for the separation of broad ultrahigh-molecular-weight polymers [20,21]. However, the FI-AF4 system requires a high-speed frit flow (normally 20 times faster than the sample injection flow rate) and a high crossflow rate to ensure hydrodynamic relaxation of sample components. Therefore, the available range of outflow rates in FI-AF4 is limited. To analyze sample materials with a broad size distribution, selection of a proper run condition to ensure hydrodynamic relaxation and to avoid steric transition is required. However, the effect of field programming on steric transition in particle separation has not been examined in FI-AF4, which is useful for the separation/isolation of biological particles and the further analysis of biologically active components in conjunction with proteomic and metabolomics [22].

In the present study, the effect of field programming on steric transition in FI-AF4 has been investigated with PS latex particles. By varying the field decay patterns, the rate ratio of frit flow to injection flow, initial field strength, and channel thickness, a possible extension of steric transition to a larger diameter scale has been achieved.

2. Theory

The retention ratio, R, is defined as the ratio of void time, t°, to retention time, t_r, and R in the normal mode is generally expressed as

$$R = \frac{t^0}{t_r} = 6\lambda\left[\coth\left(\frac{1}{2\lambda}\right) - 2\lambda\right] \quad (1)$$

where λ is the ratio of mean layer thickness of the sample zone to the channel thickness, w, which is given for FlFFF as

$$\lambda = \frac{D}{Uw} = \frac{kT}{3\pi\eta wUd} \quad (2)$$

where D is the diffusion coefficient of the sample component (= $kT/3\pi\eta d$), U is the transverse flow velocity of the crossflow, k is Boltzmann distribution constant, T is absolute temperature, η is the viscosity of the carrier liquid, and d is the particle diameter. In the case of a small λ, Eq. (1) can be simply expressed as

$$R = 6\lambda = \frac{2kT}{\pi\eta wUd} = \frac{2kTV^0}{\pi\eta w^2 d\dot{V}_c} \quad (3)$$

where V° is the channel void volume and $\dot{V}_c$ is the volumetric flow rate of crossflow (=A_cU, where A_c is the total area of the accumulation wall) [1,2,23]. However, in the steric/hyperlayer mode of FlFFF, the retention ratio is expressed as

$$R = \frac{t^0}{t_r} = \frac{3\gamma d}{w} \quad (4)$$

where γ is the steric correction factor, which depends on the field strength, migration flow velocity, and particle diameter [24]. Owing to the complicated properties of hydrodynamic lift forces, γ has not been fully resolved and thus, retention in the steric/hyperlayer mode cannot be theoretically expected [25]. Instead, a calibration is normally applied to determine the particle diameter from the retention time [12,23] as

$$\log t_r = \log t_{r1} - S\log d \quad (5)$$

where t_{r1} is the extrapolated retention time of a unit diameter and S (>0) is the diameter-based selectivity in the steric/hyperlayer separation. Therefore, the retention ratio can be written as the sum of Eqs. (3) and (4) as

$$R = \frac{t^0}{t_r} = 6\lambda + \frac{3\gamma d}{w} \quad (6)$$

and it can be expressed by using the calibration equation in Eq. (5) as

$$R = \frac{2kT}{\pi\eta wUd} + \frac{t^0}{t_{r1}}d^S \quad (7)$$

From Eq. (7), the steric inversion diameter, d_i, can be semi-empirically determined at $\frac{\partial R}{\partial d} = 0$ [13,26] as follows:

$$d_i = \left(\frac{2kTt_{r1}}{\pi\eta wUt^0 S}\right)^{\frac{1}{S+1}} \quad (8)$$

Eq. (8) applies to a typical FlFFF channel with an appropriate equation of t° according to the channel type (symmetrical, asymmetrical, and frit-inlet asymmetrical FlFFF). For a frit-inlet asymmetrical FlFFF (FI-AF4) channel, t° can be expressed in a reduced form as [19]

$$t^0 = \frac{V^0}{\dot{V}_c}\left\{\frac{\dot{V}_s}{\dot{V}_f - \dot{V}_s} ln\left(\frac{\dot{V}_f}{\dot{V}_s}\right) + ln\left(\frac{\dot{V}_f}{\dot{V}_{out}}\right)\right\} \text{ (for FI} - \text{AF4)} \quad (9)$$

where $\dot{V}_s$ is the injection flow rate, $\dot{V}_f$ is the frit flow rate, and $\dot{V}_{out}$ is the outflow rate leading to the detector. Eq. (9) is valid only when $\dot{V}_s \le \dot{V}_f A_f/A_c$, where A_f is the area of the inlet frit. Eq. (8) indicates that the steric inversion diameter can be increased with a decrease in U at a given channel thickness, but can be, to some degree, offset by the decrease in t_{r1} in the steric/hyperlayer separation. When utilizing the field programming in the FlFFF channel, an additional decrease in void time, which is a function of time as $t^\circ(t)$, along with a decrease in the slope (S) of steric calibration may result in an increase in the steric inversion diameter. When field programming

is introduced, U and t° in Eq. (8) are no longer constants as $U(t)$ (= $\dot{V}_c(t)/A_c$) and $t^{\circ}(t)$ at time t. For instance, the crossflow rate in a linear decay pattern can be expressed as [27]

$$\dot{V}_c(t) = \dot{V}_{c0} - \Delta\dot{V}_c\left(\frac{t-t_1}{t_p}\right) \quad (10)$$

where $\dot{V}_{c0}$ is the initial crossflow rate, $\Delta\dot{V}_c$ is the decrease in the crossflow rate during the program, t_1 is the initial time delay before the field decay begins, and t_p is the transient time for programming. When the crossflow rate is varied by fixing $\dot{V}_{out}$, the void time in Eq. (9) becomes

$$t^0(t) = \frac{V^0}{\dot{V}_c(t)}\left\{\frac{\dot{V}_s}{\dot{V}_f(t)-\dot{V}_s} ln\left(\frac{\dot{V}_f(t)}{\dot{V}_s}\right) + ln\left(\frac{\dot{V}_f(t)}{\dot{V}_{out}}\right)\right\}$$

(for FI – AF4 with field decay) (11)

This will require a complicated numerical calculation for the prediction of steric inversion diameter in the normal mode, which is beyond the scope of this study. However, it will be useful to attempt an experimental approach to increase the steric inversion diameter by utilizing field programming at different channel thicknesses. The present study will investigate the possibility of increasing the steric inversion diameter by utilizing the FI-AF4 channel system.

3. Experimental

PS latex standards were purchased from Thermo Fisher Scientific (Waltham, MA, USA) and their nominal diameters were 0.046, 0.102, 0.203, 0.303, 0.400, 0.498, 0.702, 0.799, 0.903, 0.994, 1.999, 4.000, 6.007, 7.979, and 10.15 μm. Hereafter, they are referred to as 50, 100, 200, 300, 400, 500, 700, 800, and 900 nm and 1, 2, 4, 6, 8, and 10 μm, respectively. Sodium dodecyl sulfate (SDS) and NaN_3 were purchased from Sigma-Aldrich (St. Louis, MO, USA).

The FI-AF4 channel utilized in this study was modified from a model LC channel from Wyatt Technology Europe GmbH (Dernbach, Germany) by replacing the depletion wall block with a polycarbonate block embedded with a ceramic frit (35 mm × 18 mm × 7 mm) in our laboratory. The installation of an inlet frit with plumbing is described in literature [28]. Channel spacers were cut from Mylar sheets with different thicknesses of 190, 350, and 490 μm with a tip-to-tip length of 26.6 cm and an inlet width of 2.2 cm with a trapezoidal decrease to an outlet width of 0.6 cm A regenerated cellulose membrane with a pore size of 20 kDa, obtained from Merck Millipore (Darmstadt, Germany), was utilized at the accumulation wall. The carrier solution was prepared using ultrapure water (>18 MΩ•cm) added with 0.05% SDS and 0.02% NaN_3 as a bactericide. The prepared solution was filtered with Durapore® hydrophilic polyvinylidene fluoride membrane filter (pore size 0.1 μm) obtained from Merck Millipore and degassed 1 h prior to the FI-AF4 analysis. Sample injection was performed using a model 7725i loop injector from Rheodyne (Cotati, CA, USA) with a sample loop (6 μL) through the sample inlet using SP930D high-performance liquid chromatography (HPLC) pump from Young-Lin Instruments (Seoul, Korea). PS particles of submicrometer sizes were diluted with the carrier liquid (×10 for 50 nm, ×60 for 100 nm, ×100 for 200–500 nm, ×10 for 600–900 nm) and supramicron-sized PS particles were used without dilution. All injections were performed with 1 μL of each standard. The frit flow was delivered to the inlet frit port using a model 1260 Infinity HPLC pump from Agilent Technologies (Palo Alto, CA, USA), controlled by the Eclipse Separation System for AF4 from Wyatt Technology Europe GmbH. The Eclipse system controlled both the outflow rate and crossflow rate, which was programmed to decrease linearly during the separation. During field programming, the crossflow rate was

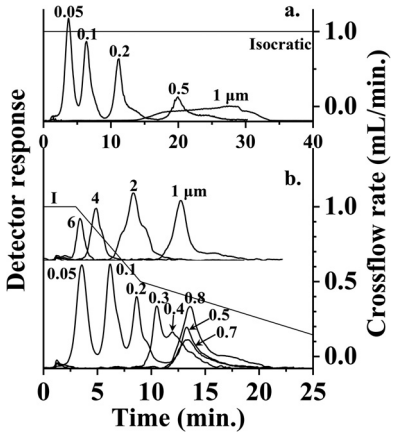

Fig. 1. Fractograms of polystyrene (PS) particles in FI-AF4 (w = 190 μm) using a) constant field strength ($\dot{V}_c$ = 1.0 mL/min) and b) a linear field programming (the decay-I). $\dot{V}_s$ = 0.1 mL/min, $\dot{V}_{out}$ = 0.7 mL/min, and $\dot{V}_f$ was adjusted as $\dot{V}_c + \dot{V}_{out} - \dot{V}_s$.

1.0 mL/min initially for the decay-I and was maintained for 3 min; it was thereafter decreased to 0.5 mL/min for 6 min, to 0.1 mL/min for 18 min, further to 0.02 mL/min for 6 min, and was thereafter maintained at 0.02 mL/min. The decay-II began with a higher initial crossflow rate of 3.0 mL/min but the decay patterns were the same as those of the decay-I. The eluted PS particles were monitored at a wavelength of 254 nm using a model UV730D UV–vis detector from Young-Lin Instruments. The detector signals were recorded using ASTRA software from Wyatt.

4. Results & discussion

The effect of field programming on the separation of PS latex standards in an FI-AF4 channel system is compared with that of an isocratic (constant field) run in Fig. 1. In the constant crossflow rate condition, submicron PS particles were reasonably separated, except for the particles of size 1 μm, which were not successfully resolved. The flow rates employed were $\dot{V}_s$ = 0.1, $\dot{V}_{out}$ = 0.7, the initial $\dot{V}_c$ = 1.0 mL/min, which was constant in Fig. 1a and decreased linearly (the decay-I) in Fig. 1b, and $\dot{V}_f$ varied with the decrease in crossflow rate as $\dot{V}_f + \dot{V}_s = \dot{V}_c + \dot{V}_{out}$ in an FI-AF4 channel system. The thickness of the channel spacer employed in Fig. 1 was 190 μm. When field programming was applied to Fig. 1b, the elution times of submicron particles were reduced with some loss of resolution. The separation of supramicron-sized PS particles was achieved in a decreasing order of sizes. Although PS particles during field programming eluted without a serious band broadening, particles in the size range 0.5–1 μm were not yet resolved from each other owing to the combination of normal and steric/hyperlayer modes of retention. As the separation was achieved in a relatively thin channel (w = 190 μm), the contribution of lift forces can be significant and the decrease in field strength during field programming may not reduce the steric/hyperlayer effect as much as expected. At the elution time of particles in the steric transition region, it appears that the steric inversion diameter was in the range 0.7–0.8 μm.

To minimize the contribution of the lift force, steric transition was investigated with a channel of increased thickness (w = 350 μm). Fig. 2 shows the comparison of particle separation between a) the isocratic field and b) linear field decay (the decay-I). The flow rate conditions were the same as those used in Fig. 1. Fig. 2a demonstrates that an increase in the channel thickness enhanced the separation resolution, but with a substantial broadening of all the eluting components. In the constant field strength condition, supramicron particles were not successfully resolved owing

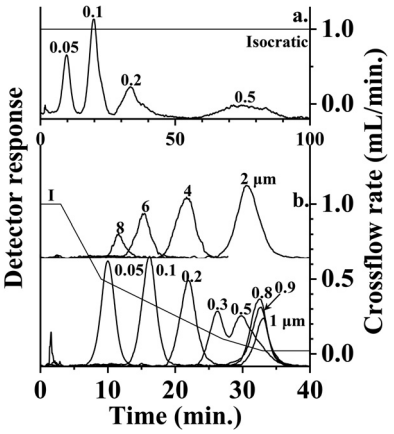

Fig. 2. Separation of PS standards in FI-AF4 with a channel of increased thickness (w = 350 μm) using a) constant field strength ($\dot{V}_c$ = 1.0 mL/min) and b) field decay pattern I. $\dot{V}_s$ = 0.1 mL/min, $\dot{V}_{out}$ = 0.7 mL/min.

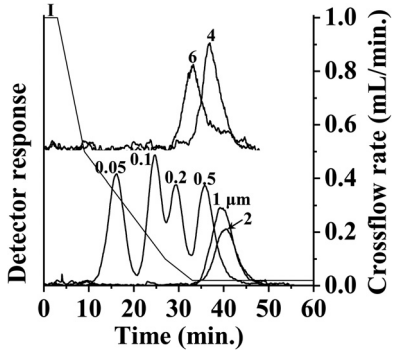

Fig. 4. Field programming in the FI-AF4 separation of PS particles with a channel (w = 490 μm). $\dot{V}_s$ = 0.1 mL/min and $\dot{V}_{out}$ = 0.7 mL/min.

to the reduced migration flow velocity. The employment of field programming in the 350-μm-thick channel resulted in a successful separation of supramicron particles in Fig. 2b and improved the normal mode separation in which the resolution of particles of sizes 0.5 and 0.8 μm was better than that observed in Fig. 1b. Moreover, the retention time (33.1 min) of particles of size 1 μm in a thicker channel appeared to be longer than that (29.8 min) of particles of size 0.5 μm, confirming that the steric transition was increased to a larger diameter scale. With the thinner channel in Fig. 1b, the particles of size 1 μm eluted earlier than those of size 0.5 μm.

The influences of the experimental parameters in FI-AF4 channels on the separation of PS latex standards were further investigated. Fig. 3a shows the normal mode of separation by linear field programming (the decay-I) obtained by increasing the outflow rates from 0.4 to 1.0 mL/min while $\dot{V}_s$ was fixed at 0.1 mL/min. As the frit flow rate ($\dot{V}_f$) is equal to $\dot{V}_c + \dot{V}_{out} - \dot{V}_s$, the initial $\dot{V}_f$ values should be 1.3, 1.6, and 1.9 mL/min for the top, middle, and bottom fractograms in Fig. 3a, respectively. An increase in the outflow rate in FI-AF4 under the same field decay pattern requires an increase in the frit flow, which increases the migration speed of particles during the hydrodynamic relaxation. The shoulder before the particle elution at the top of Fig. 3a is caused by the surged elution of some particles originating from incomplete hydrodynamic relaxation under a low ratio of $\dot{V}_f/\dot{V}_s$ (= 1.3/0.1). In an earlier report, this ratio was determined to be effective when it was close to 20 [18]. However, for the case of the bottom fractogram, which employed a sufficiently high $\dot{V}_f$ (= 1.9 mL/min), it did not lead to a successful separation as the outflow rate (1.0 mL/min) was too high. When the initial field strength was raised to 3.0 mL/min (the decay-II) in the top fractogram of Fig. 3b in comparison with the decay-I with the fixed $\dot{V}_s$ = 0.1 and $\dot{V}_{out}$ = 0.7 mL/min, it did not make a significant difference in the separation of late eluting particles (> 0.2 μm) as the field decay patterns after 10 min of run were the same.

A further increase in the channel thickness to w = 490 μm resulted in a shift in the steric transition region to a larger diameter scale as PS particles of size 2 μm eluted slightly later than those of size 1 μm in Fig. 4 whereas their retention order was reversed in Fig. 2. Notably, the band broadening was significantly increased as the flow rate conditions were the same as those used in Fig. 2, resulting in a substantial decrease in the migration speed with an increase in the channel thickness. However, it can be useful that the steric transition region can be shifted to a large diameter scale when the field programming is employed with an increase in the channel thickness in FlFFF. The steric inversion diameter, d_i, at different channel thicknesses can be simply estimated from the experimental relationship between the retention time and particle diameter as shown in Eq. (5), which can be separately established for both normal and steric/hyperlayer modes. Fig. 5 shows the plots of log t_r (min) vs. log d (μm) of PS particles measured with the channels of the three different thicknesses (190, 350, and 490 μm). The

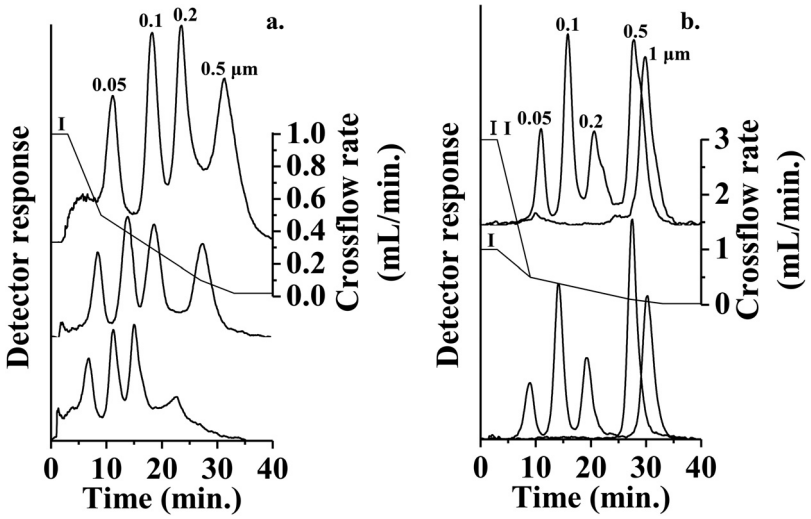

Fig. 3. Effects of a) $\dot{V}_{out}$ (0.4, 0.7, and 1.0 mL/min from the top) and b) the initial field strength ($\dot{V}_c$ = 3.0 mL/min for the top and 1.0 mL/min for the bottom, $\dot{V}_{out}$ = 0.7 mL/min for both) on programmed-field separation of PS latex standards in FI-AF4 (w = 350 μm). $\dot{V}_s$ = 0.1 mL/min for all runs.

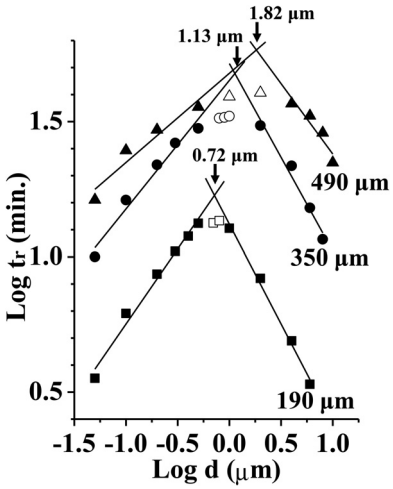

Fig. 5. Plots of log t_r (min) vs. log d (μm) of PS particles obtained by programmed-field separation in FI-AF4 at different channel thicknesses (190, 350, and 490 μm).

Table 1
Slope and intercept values of the calibration plots of log t_r (min) vs. log d (μm) of PS latex particles for the three different channel thicknesses shown in Fig. 5. Data points marked with filled symbols in Fig. 5 were included to establish the calibration curves in Eq. (5).

w (mm)	Normal mode			Steric/hyperlayer mode		
	S_N	log t_{r1} (min)	R^2	S	log t_{r1} (min)	R^2
190	0.55	1.31	0.986	0.74	1.12	0.994
350	0.48	1.65	0.972	0.69	1.71	0.975
490	0.33	1.68	0.928	0.52	1.90	0.893

steric inversion diameter can be empirically estimated from the calibration parameters of both normal and steric/hyperlayer modes as listed in Table 1 without referring to Eq. (8) as the semi-empirical approach used to determine d_i in Eq. (8) requires a numerical calculation of void time varied during the field programming as in Eq. (11). Fig. 5 shows that d_i can be increased by employing field programming in FlFFF. The typical steric inversion diameter in FlFFF was determined to be ~ 0.5 μm, but it was increased to 0.72 μm at the channel with w = 190 μm in Fig. 5 and to a value as large as 1.8 μm with an increased channel thickness (w = 490 μm). Notably, the slope values (S) in Table 1 or the diameter selectivity was observed to decrease with the application of field programming. In Table 1, the slope values of the steric/hyperlayer mode followed the expression of S in Eq. (5); however, the slope of the normal mode, S_N, followed log t_r = log t_{r1} + S_N log d.

5. Conclusion

The steric transition phenomena in FI-AF4 channel systems have been investigated by employing field programming and increasing the channel thickness. As the steric inversion diameter of any FlFFF channel system was observed to be approximately 0.5 μm, FlFFF separation of particulate materials covering this size is limited. The present study demonstrated that the steric inversion diameter could be increased to above 1 μm when the crossflow rate was programmed to decrease with the increase in channel thickness. The steric inversion diameter was observed to increase to 1.8 μm with a 490-μm-thick channel; however, separation resolution was sacrificed to some degree owing to the increase in band broadening. The results of this study suggested that field programming with the 350-μm-thick channel can be useful to improve the normal mode of separation to as close as 1 μm without a serious increase in the retention time. As the FI-AF4 channel system requires a high rate of frit flow to ensure successful hydrodynamic relaxation of sample components, the possible range of outflow rates is limited; therefore, field programming with the application of a higher frit flow rate can be an alternative to successfully operate an FI-AF4 channel. The present study demonstrated that steric transition in the FI-AF4 channel can be extended to a large diameter scale to some degree by utilizing crossflow programming at an increased channel thickness, which can be useful to separate particles without encountering steric transition at the submicron level.

Acknowledgements

This study was supported by the grant NRF-2018R1A2A1A05019794 from the National Research Foundation (NRF) of Korea.

References

[1] J.C. Giddings, Field flow fractionation - a versatile method for the characterization of macromolecular and particulate materials, Anal. Chem. 53 (1981) 1170–1178, http://dx.doi.org/10.1021/ac00234a001.
[2] J.C. Giddings, Field-flow fractionation: analysis of macromolecular, colloidal, and particulate materials, Science 260 (1993) 1456–1465, http://dx.doi.org/10.1126/science.8502990.
[3] J.C. Giddings, F.J. Yang, M.N. Myers, Flow-field-flow fractionation: a versatile new separation method, Science 193 (1976) 1244–1245, http://dx.doi.org/10.1126/science.959835.
[4] K.G. Wahlund, H.S. Winegarner, K.D. Caldwell, J.C. Giddings, Improved flow field-flow fractionation system applied to water-soluble polymers: programming, outlet stream splitting, and flow optimization, Anal. Chem. 58 (1986) 573–578, http://dx.doi.org/10.1021/ac00294a018.
[5] M. Nilsson, L. Bulow, K.G. Wahlund, Use of flow field-flow fractionation for the rapid quantitation of ribosome and ribosomal subunits in Escherichia coli at different protein production conditions, Biotechnol. Bioeng. 54 (1997) 461–467, http://dx.doi.org/10.1002/(SICI)1097-0290(19970605)54:5<461::AID-BIT6>3.0.CO;2-C.
[6] S.K. Ratanathanawongs, I. Lee, J.C. Giddings, Separation and characterization of 0.01-50-Mu-M particles using flow field-flow fractionation, ACS Symp. Ser. 472 (1991) 229–246, http://dx.doi.org/10.1021/bk-1991-0472.ch015.
[7] P. Reschiglian, A. Zattoni, B. Roda, S. Casolari, M.H. Moon, J. Lee, J. Jung, K. Rodmalm, G. Cenacchi, Bacteria sorting by field-flow fractionation. Application to whole-cell Escherichia coil vaccine strains, Anal. Chem. 74 (2002) 4895–4904, http://dx.doi.org/10.1021/ac020199t.
[8] D. Kang, M.H. Moon, Development of non-gel-based two-dimensional separation of intact proteins by an on-line hyphenation of capillary isoelectric focusing and hollow fiber flow field-flow fractionation, Anal. Chem. 78 (2006) 5789–5798, http://dx.doi.org/10.1021/ac0606958.
[9] J.S. Yang, J.Y. Lee, M.H. Moon, High speed size sorting of subcellular organelles by flow field-flow fractionation, Anal. Chem. 87 (2015) 6342–6348, http://dx.doi.org/10.1021/acs.analchem.5b01207.
[10] J.Y. Kim, H.B. Lim, M.H. Moon, Online miniaturized asymmetrical flow field-flow fractionation and inductively coupled plasma mass spectrometry for metalloprotein analysis of plasma from patients with lung Cancer, Anal. Chem. 88 (2016) 10198–10205, http://dx.doi.org/10.1021/acs.analchem.6b02775.
[11] J.C. Giddings, Retention (Steric) inversion in Field-Flow fractionation - practical implications in Particle-Size, density and shape-analysis, Analyst 118 (1993) 1487–1494, http://dx.doi.org/10.1039/AN9931801487.
[12] J.C. Giddings, M.H. Moon, P.S. Williams, M.N. Myers, Particle size distribution by sedimentation/steric field-flow fractionation: development of a calibration procedure based on density compensation, Anal. Chem. 63 (1991) 1366–1372, http://dx.doi.org/10.1021/ac00014a006.
[13] M.H. Moon, J.C. Giddings, Extension of sedimentation steric field-flow fractionation into the submicrometer range - size analysis of 0.2-15-Mu-M metal particles, Anal. Chem. 64 (1992) 3029–3037, http://dx.doi.org/10.1021/ac00014a006.
[14] K.D. Jensen, S.K. Williams, J.C. Giddings, High-speed particle separation and steric inversion in thin flow field-flow fractionation channels, J. Chromatogr. A 746 (1996) 137–145, http://dx.doi.org/10.1016/0021-9673(96)00288-9.
[15] H. Dou, Y.J. Lee, E.C. Jung, B.C. Lee, S. Lee, Study on steric transition in asymmetrical flow field-flow fractionation and application to characterization of high-energy material, J. Chromatogr. A 1304 (2013) 211–219, http://dx.doi.org/10.1016/j.chroma.2013.06.051.
[16] M.H. Moon, K.H. Lee, B.R. Min, Effect of temperature on particle separation in hollow fiber flow field-flow fractionation, J. Microcolumn Sep. 11 (1999) 676–681, http://dx.doi.org/10.1002/(SICI)1520-667X(199911)11:9<676::AID-MCS5>3.0.CO;2-O.
[17] H. Lee, J.Y. Kim, W. Choi, M.H. Moon, Effect of cationic monomer content on polyacrylamide copolymers by frit-inlet asymmetrical flow field-flow

fractionation/multi-angle light scattering, J. Chromatogr. A 1503 (2017) 49–56, http://dx.doi.org/10.1016/j.chroma.2017.04.057.
[18] M.H. Moon, H. Kwon, I. Park, Stopless flow injection in asymmetrical flow field-flow fractionation using a frit inlet, Anal. Chem. 69 (1997) 1436–1440, http://dx.doi.org/10.1021/ac960897b.
[19] M.H. Moon, P.S. Williams, H. Kwon, Retention and efficiency in frit-inlet asymmetrical flow field-flow fractionation, Anal. Chem. 71 (1999) 2657–2666, http://dx.doi.org/10.1021/ac990040p.
[20] M. Ali, E. Hwang, I.H. Cho, M.H. Moon, Characterization of sodium hyaluronate blends using frit inlet asymmetrical flow field-flow fractionation and multiangle light scattering, Anal. Bioanal. Chem. 402 (2012) 1269–1276, http://dx.doi.org/10.1007/s00216-011-5531-0.
[21] S. Woo, J.Y. Lee, W. Choi, M.H. Moon, Characterization of ultrahigh-molecular weight cationic polyacrylamide using frit-inlet asymmetrical flow field-flow fractionation and multi-angle light scattering, J. Chromatogr. A 1429 (2016) 304–310, http://dx.doi.org/10.1016/j.chroma.2015.12.027.
[22] M.H. Moon, Frit-inlet asymmetrical flow field-flow fractionation (FI-AFIFFF): a stopless separation technique for macromolecules and nanoparticles, Bull. Korean Chem. Soc. 22 (2001) 337–348.
[23] S.K. Ratanathanawongs, J.C. Giddings, Dual-field and flow-programmed lift hyperlayer field-flow fractionation, Anal. Chem. 64 (1992) 6–15, http://dx.doi.org/10.1021/ac00025a003.
[24] M.N. Myers, J.C. Giddings, Properties of the transition from normal to steric field-flow fractionation, Anal. Chem. 54 (1982) 2284–2289, http://dx.doi.org/10.1021/ac00250a032.
[25] R.E. Peterson, M.N. Myers, J.C. Giddings, Characterization of steric field-flow fractionation using particles to 100 Mu-M diameter, Separ. Sci. Technol. 19 (1984) 307–319, http://dx.doi.org/10.1080/01496398408068585.
[26] B.R. Min, S.J. Kim, K.H. Ahn, M.H. Moon, Hyperlayer separation in hollow fiber flow field-flow fractionation: effect of membrane materials on resolution and selectivity, J. Chromatogr. A 950 (2002) 175–182, http://dx.doi.org/10.1016/S0021-9673(02)00029-8.
[27] M.H. Moon, P.S. Williams, D.J. Kang, I. Hwang, Field and flow programming in frit-inlet asymmetrical flow field-flow fractionation, J. Chromatogr. A 955 (2002) 263–272, http://dx.doi.org/10.1016/S0021-9673(02)00226-1.
[28] B. Kim, S. Woo, Y.S. Park, E. Hwang, M.H. Moon, Ionic strength effect on molecular structure of hyaluronic acid investigated by flow field-flow fractionation and multiangle light scattering, Anal. Bioanal. Chem. 407 (2015) 1327–1334, http://dx.doi.org/10.1007/s00216-014-8379-2.